EUROPEAN ORGANIZATION FOR NUCLEAR RESEARCH
CERN - ACCELERATORS AND TECHNOLOGY SECTOR

CERN-ATS 2012-287

Carbon Coatings with Low Secondary Electron Yield

P. Costa Pinto, S. Calatroni, H. Neupert, D. Letant-Delrieux, P. Edwards, P. Chiggiato,
M. Taborelli, W.Vollenberg, C. Yin-Vallgren,
CERN, Geneva, Switzerland

J. Colaux, S. Lucas
Centre de Recherche en Physique de la Matière et du Rayonnement (PMR),
LARN Laboratory - University of Namur (FUNDP), Belgium

Carbon thin films for electron cloud mitigation and anti-multipacting applications have been prepared by dc magnetron sputtering in both neon and argon discharge gases and by plasma enhanced chemical vapour deposition (PECVD) using acetylene. The thin films have been characterized using Secondary Electron Yield (SEY) measurements, Scanning Electron Microscopy (SEM), Nuclear Reaction Analysis (NRA) and X-ray Photoelectron Spectroscopy (XPS). For more than 100 carbon thin films prepared by sputtering the average maximum SEY is 0.98+/-0.07 after air transfer. The density of the films is lower than the density of Highly Ordered Pyrolytic Graphite (HOPG), a fact which partially explains their lower SEY. XPS shows that magnetron sputtered samples exhibit mainly sp^2 type bonds. The intensity on the high binding energy side of C1s is found to be related to the value of the SEY. Instead the initial surface concentration of oxygen has no influence on the resulting SEY, when it is below 16%. The thin films produced by PECVD have a much higher maximum SEY of 1.49+/-0.07.
Storage conditions in air, namely wrapping in aluminium foil, preserves the low SEY by more than one year. Such coatings have already been applied successfully in accelerators and multipacting test benches.

Presented at the 12th European Vacuum Conference (EVC'14)
4-8 June 2012, Dubrovnik, Croatia

Genève, Suisse

November 2012

1. Introduction

Low Secondary Electron Yield (SEY) materials are required to avoid multipacting in RF devices in space [1] and the electron-cloud effect in high intensity particle accelerators that use positively charged beams [2, 3]. Ideally all these phenomena based on electron multiplication are suppressed if the SEY is lower than 1.0, however in practice, depending on geometry and magnetic field conditions, the threshold level is often slightly higher than unity. Since the SEY is a quantity related to the topmost 3-5 nm layer of the material [4], an appropriate modification of the surface properties is sufficient to reduce its value.

Pure metal surfaces usually have low SEY (about 1.3), but air exposure makes the SEY increase up to 2.0 [5]. Surface cleaning for components inserted in Ultra High Vacuum (UHV) is therefore beneficial. Cleaning processes before installation (detergent or solvent cleaning) or in situ under vacuum (plasma discharge, bake-out), which remove the airborne contamination can be applied. However, these treatments do not prevent recontamination upon prolonged air exposure, as for instance for maintenance. Other effective processes include treatments which induce surface roughness [6] or coating with a thin film of intrinsically low SEY [7, 8].

Non-evaporable getters (NEG) are a special type of coatings, which have a strong decrease in SEY after thermal activation in UHV at a temperature higher than 180°C [7]. NEG is successfully applied in most of the room temperature sections of the Large Hadron Collider (LHC) [9]. In some situations, such as in the case of the Super Proton Synchrotron (SPS) at CERN or in space applications, thermal activation is not possible because of limitations imposed by the constituent materials of the systems or the available power. Unfortunately some of the coatings which nominally do not need

thermal activation, e.g. TiN, are sufficiently reactive in air to form an oxidized layer which partly cancels the benefit of the originally low SEY [10, 11].

The main aim of the work presented here was to produce a thin film coating with a reliable low initial SEY, that does not require in-situ bake-out and is robust against air exposure. From several earlier studies, carbon and carbon nitrides are known to have a low SEY [1, 12, 13, 14] and the formation of a layer of carbon is generally believed to be the responsible for the conditioning effect occurring in accelerators [15, 16]. In this work, carbon coatings have been produced by dc magnetron sputtering (MS) and Plasma Enhanced Chemical Vapor Deposition (PECVD). The development of the coatings was driven by the low SEY as the main quantity to accept or discard the production method. In addition the coatings were characterized for their surface chemical composition by X-Ray Photoelectron Spectroscopy (XPS), Nuclear Reaction Analysis (NRA) was used to estimate the bulk density and Scanning Electron Microscopy (SEM) to characterize the morphology. Coatings of this type prepared by MS have already been successfully tested in the SPS for mitigation of electron cloud [17].

2. Materials and methods for carbon coatings:

The investigated samples are thin film coatings of 50-2000 nm thickness deposited by dc MS, using graphite cathodes placed in the center of a cylindrical or hippodrome cross-section vacuum chambers with a minimum diameter in the range 50-159 mm. Typically the length of the vacuum chamber to be coated ranged from 500 to 6500 mm. The magnetic field was applied by a solenoid along the chamber axis (150 Gauss). For all the properties presented in the following no systematic differences are found between the various geometries. Stainless steel bands of about 20 mm width and 0.5-1

mm thickness were placed in the chambers after standard cleaning for ultrahigh vacuum (UHV) [18] and were used as coating substrate for investigation of SEY, XPS and SEM.

For other measurements, such as NRA, silicon and copper substrates were also used. Neon was selected as the discharge gas for most of the coatings (111 samples), referred hereafter as CNe, and few samples (8) were prepared with argon, referred hereafter as CAr.

Before the coatings, the system was in most cases unbaked and the typical base pressure was in the range of 10^{-8} mbar. Bake out at 300C during one night was performed generally for long vacuum chambers. The pressure on the pump side of the chamber was in such cases 10^{-9} mbar range. No external heating was applied during coating and the substrate temperature was left free to vary due to the discharge power. From measurements (thermocouples) and calculations – in the cases where it was not possible to place thermocouples in the vacuum side- the maximum temperature during coating remained below 300C. The range of parameters used in the present study are given in table 1.

The Plasma Enhanced Chemical Vapour Deposition (PECVD) coatings were performed by using C_2H_2 as the precursor gas (99% purity) and deposited on stainless steel substrates. In this process a bias dc voltage is applied to a central anode of stainless steel placed along the axis of the vacuum chamber to produce the plasma. The pressure of the C_2H_2 is adjusted through a leak valve and is maintained constant by pumping through a low conductance by-pass. In total 6 PECVD coatings were prepared and investigated.

Many coatings were tested for adhesion by using the common scotch tape test and did not shown peel off under visual inspection. Any production of dust particles was monitored by a particle counter (down to 3 microns size) by comparing the result in a coated and in a bare stainless steel vacuum pipe, which was cleaned with the procedure for UHV parts. No significant difference was found between the two cases. The experiment was repeated also after gently hitting on the chamber wall on the external side with a hammer and the result was the same.

Table 1: Range of coating parameters used in the present investigation

Method	**Voltage**	**Power per unit length [W/m]**	**Pressure [mbar]**	**Deposition rate**
Ne MS	700 – 800	200 W	$5.7 – 7.6 \times 10^{-2}$	depending on geometry
Ar MS	700 – 800	200 W	3.8×10^{-2}	depending on geometry
C_2H_2 PECVD	400 - 1300	50 – 1400W	$1.0 – 3.0 \times 10^{-1}$	25 nm/min @ 50W

In addition a pure graphite sample (Goodfellow Metals) of Highly Oriented Pyrolithic Graphite (HOPG) was used as a reference to compare the SEY values and XPS spectra. Before measurements in XPS and SEY this sample was cleaved in air. In this way SEY of the coatings can be compared to measurements made in any instrumental setup having a different geometry.

For some of the MS coatings the deposition chamber was connected through a small conductance to a further vacuum chamber, which can be pumped by a separate turbo-molecular pumping system and hosts a residual gas analyzer (RGA). This set up enables a relatively low pressure compared to the high pressure of the discharge chamber in the 10^{-2} mbar range. Thus the RGA can be operated and a relative measurement (without

absolute quantification) of the impurities in the discharge gas during the presence of the plasma in the deposition chamber can be performed.

2.1 NRA measurements:

Nuclear Reaction Analysis (NRA) combined with Elastic Recoil Detection Analysis (ERDA) and Rutherford Backscattering Spectroscopy (RBS) was performed to measure the chemical composition of the bulk of the films and calculate their density. The analysis was made with an impinging beam of 3He+ at 2.4MeV, with a typical current of 15 nA over an area of 1.5 mm in diameter. The sample under analysis was tilted to form an angle of 20° with the incident beam direction. Three PIPS (Passivated Implanted Planar Silicon) detectors were simultaneously used to perform the analysis. They were placed at 165° (RBS-detector), 90° (NRA-detector) and 30° (ERDA-detector) with respect to the incident beam direction. The RBS signal, mainly generated by the substrate (highest atomic number), was used to determine the number of incident particles and the shape of the substrate/coating interface. The NRA-detector was used to measure the protons and alpha particles emitted by (3He, p) and (3He, 4He) nuclear reactions induced on 12C and 16O. Due to the different Q-values, the NRA spectrum was composed of well separated peaks associated with these nuclear reactions. The intensity of the NRA-peaks informed us about the concentration of 12C and 16O within the deposited layer. Finally, the hydrogen particles ejected from the coating by the incident beam were collected within the ERDA-detector. The intensity of the ERDA signal was then correlated to the hydrogen content within the deposited layer. The depth profile of sample is obtained by fitting the RBS, NRA and ERDA spectra using SIMNRA [19]. This code generates a theoretical spectrum according to the experimental setup and the depth profile of the target. The aim of this analysis is then to

adjust the target depth profile in order to properly fit the RBS, NRA and ERDA experimental spectra. For that purpose, we used the SIMTarget code [20] which makes it possible to easily modify the target composition and the diffusion at the substrate/coating interface. Finally, the areal density (atoms/cm^2) of 12C, 16O and 1H can be deduced from the sample depth profile obtained by the simulations. Measuring the thickness of the deposited layer by SEM on the cross section, enables the calculation of the coating density. This technique was applied only to few samples produced by dc MS with neon. The accuracy of the thickness measurements is about 10% for coatings of 300 nm thickness.

2.2 XPS measurements*:*

In order to measure the surface chemical composition an X-ray Photoemission Spectroscopy (XPS) spectrum was usually acquired on the sample after transfer under UHV from the SEY vacuum system to the XPS system. XPS measurements were carried out using an ESCA 5400 with a non-monochromatized MgKα source. The PHI model 10-360 spherical sector electron spectrometer is operated with a fixed pass energy (fixed analyzer transmission mode). The emission angle under which the electrons are accepted by the electron spectrometer is 45°, relative to the sample normal. The analyzed sample area has a diameter of about 3 mm. The relative surface concentrations in at.%, *cx* are determined from the peak area intensitites $N(E)x$ in the XPS spectra after subtraction of a Shirley background, using the sensitivity factors $S\,x$, given in [21].

$$c_x = N(E)_x / S_x \,/ \left(\sum_i N(E)_i / S_I \right) \times 100$$

Absolute calibration of the energy scale is performed with Cu $2p^{3/2}$ and Au $4f^{7/2}$. More frequently freshly cleaved HOPG was measured to compare with the C1s line of the coatings. For a detailed analysis of the C1s line fits are performed with Gaussian components after Shirley background subtraction.

2.3 SEY measurements

The measurements of Secondary Electron Yield (SEY) were carried out with an apparatus with a similar geometry as in reference [22]. It consists of a UHV chamber, which is directly connected to the XPS vacuum system and enables transfer under UHV conditions. The chamber is equipped with an electron gun, which sends primary electrons (PE) of 80 - 2000 eV to the surface of the sample, a collector for the emitted electrons and a sample holder. The collector is biased to +45 V in order to capture all secondary electrons emitted from the sample, whereas the sample is biased to -18 V. In this geometry we measure the total SEY instead of the yield of the so-called true secondary electrons, often defined as electrons at kinetic energy below 50eV. It should be noted that the value of SEY depend also on the geometry of the collector-gun assembly used for the measurements. The vacuum system is baked and the pressure in the system is normally in the high 10^{-10} mbar region. The dimensions of the samples are in most of the cases 15 mm×15 mm×0.5-1 mm. All reported SEY measurements were carried out at normal angle of incidence. Typically values of SEY at every 50eV of primary energy were acquired. The electron dose during the measurement was calculated to be below 1×10^{-6} C/mm^2 over irradiated areas of about 2 mm^2 to give a full curve of SEY as a function of PE energy. No charging problems were encountered and the SEY curves are fully reproducible, showing that the dose has no effect. Each sample is measured on 3 different spots. Sample-to-ground current *Is* and collector-to-ground

current *Ic* are measured simultaneously by two current amplifiers and the SEY, δ, is calculated as:

$$\delta = Ic/(Ic + Is) \qquad (1)$$

where the sum of the sample current *Is* and the collector current *Ic* represents the primary current. The precision of the measured SEY values is estimated to +/- 0.03. Each sample was measured directly after extraction from the deposition chamber and transfer to the SEY measurement apparatus through air. The time in air during the transfer is approximately 4 hours. In the following the measurements on such samples will be referred to as “as received”.The most important quantities for such a measurement are the maximum SEY, called hereafter δmax and the primary energy of the maximum, called Emax.

3. Results and discussion for the as received coatings

3.1 SEY:

The results for the SEY obtained on the different coating methods are compared in figure 1, where typical curves of the yield as a function of the primary energy of the impinging electrons are displayed.

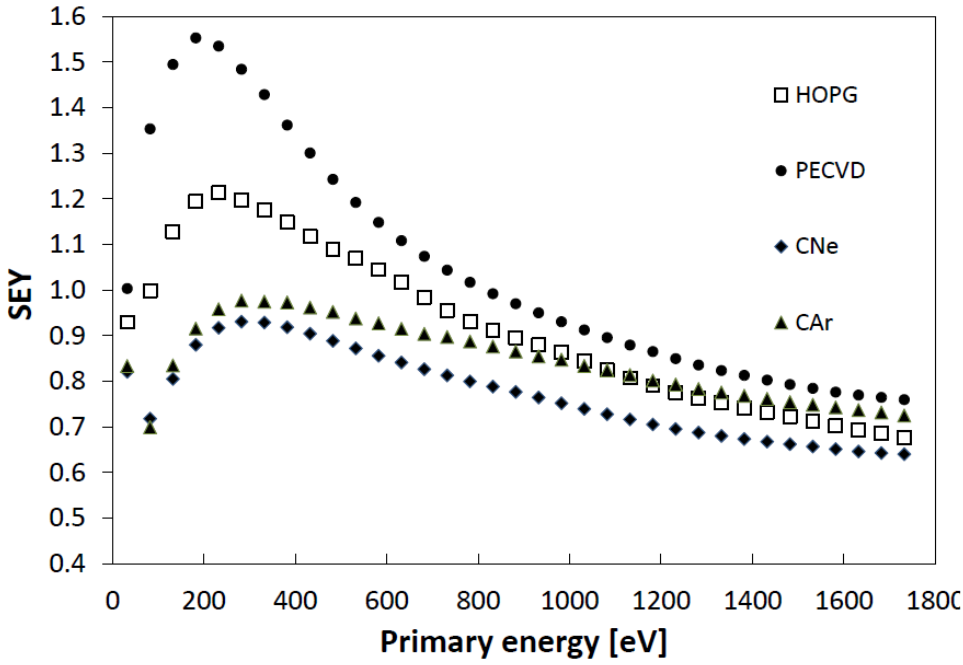

Figure1, SEY curves for coatings deposited with Ne and Ar as discharge gas, PECVD and HOPG.

In the energy range of interest the SEY of the coating deposited by MS is much lower than for HOPG, instead those produced by PECVD have a much higher SEY. The Emax values are 282eV+/-25 eV for MS, 232+/-25eV for HOPG and 181eV+/-25 eV for PECVD. The measured value of the maximum for HOPG is δmax = 1.23, which is in good agreement with reference 12, whereas other authors report lower SEY [13]. The difference in SEY between PECVD and MS is very marked as is illustrated in the histogram in figure 2, which summarizes the values of δmax for all the coatings with a thickness above 50 nm. Thinner coatings, below 50 nm, were excluded from the histogram, since they have generally a larger SEY. This fact is ascribed to secondary electrons produced in the substrate reaching the surface and being emitted.

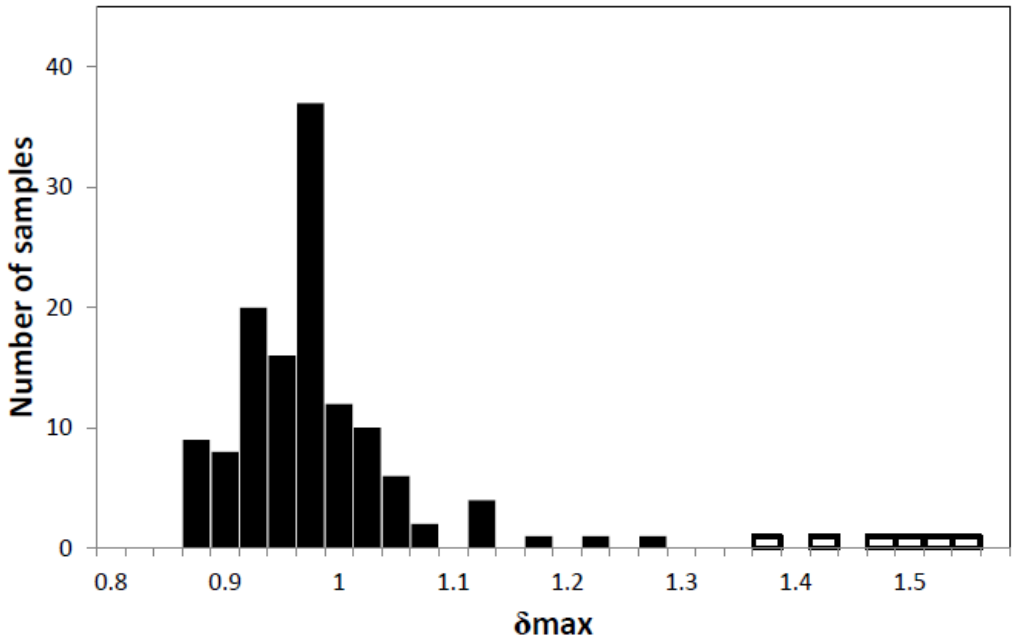

Figure 2 Histogram of δmax*, with 119 samples deposited by MS (filled black columns) and 6 samples deposited by PECVD (empty columns).*

The average δmax and the standard deviations are 0.98+/-0.07 and 1.49+/-0.07 for more than 100 samples in MS and 6 samples in PECVD, respectively. Thus the two populations are clearly separated. The narrow range of variation of δmax for the coating produced in MS - it is just about twice the precision of the measurements – makes it difficult to identify which parameters of production might influence the SEY value. Within the range of parameters of table I we do not find any systematic relationship leading to higher or lower SEY values and no difference is observed between the coatings produced with argon and those with neon. Since the typical limit of SEY for practical use in most particle accelerators is below 1.3 we did not produce more samples by PECVD based on acetylene as source gas.

3.2 Bulk composition and surface morphology:

The surface morphology of the coatings was investigated by SEM. The coatings made by MS show a tiny granularity in the 50 nm range and below (Figure 3), whereas the PECVD coatings are smoother. For the latter sample a low primary energy for imaging helps to reduce charging effects during imaging. HOPG is so smooth after cleavage (not shown) that beam focusing can only be done by using accidental surface defects, as expected for an atomically layered material.

Rougher coatings generally exhibit lower δmax and higher Emax than smoother ones. According to the SEM images, part of the difference in the δmax between HOPG and the MS deposited layers might be ascribed to roughness. The difference in Emax of the different coatings is minor (figure1), but is consistent with this argument. For PECVD instead, this argument does not hold; in spite of the larger Emax the SEY is higher compared to the one of HOPG.

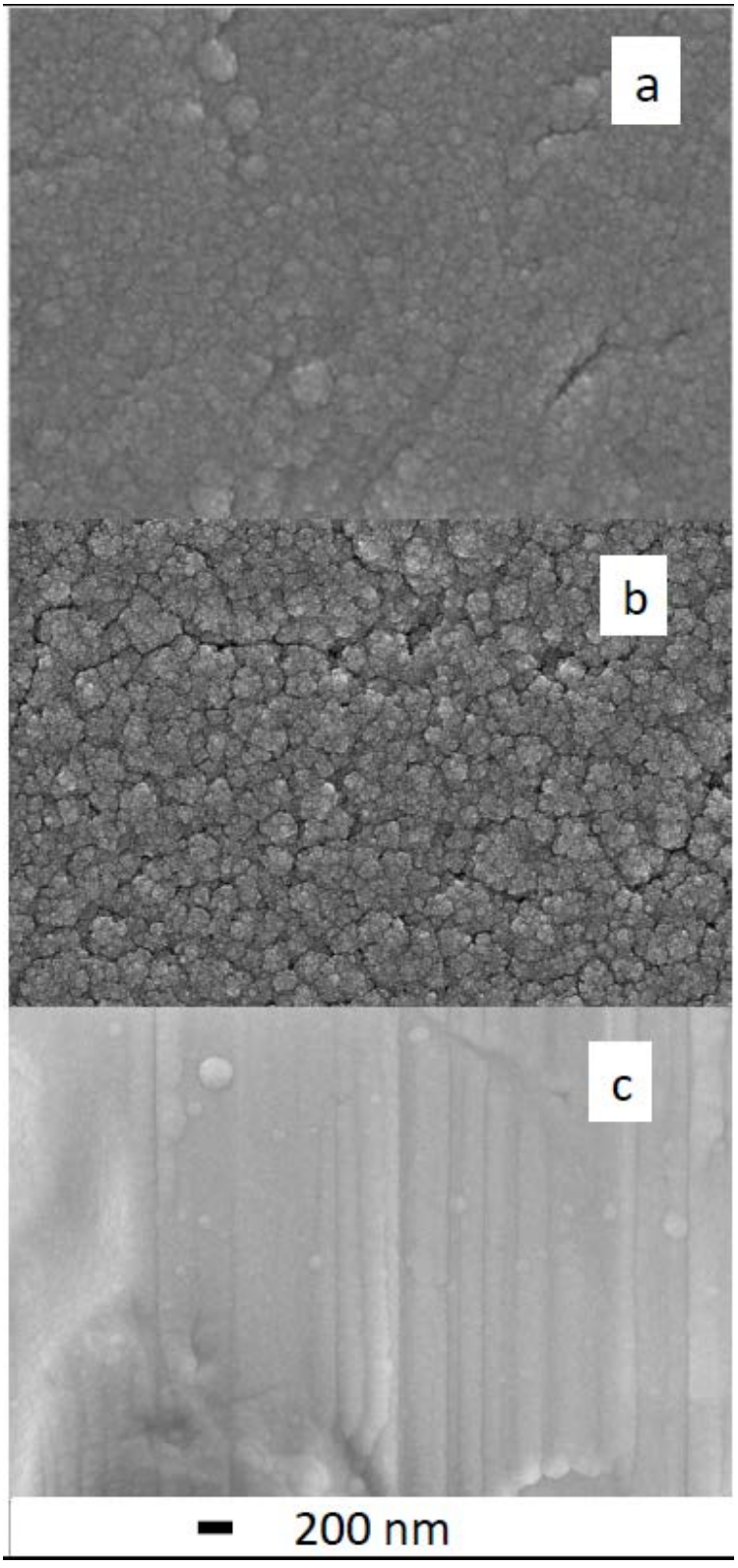

Figure 3: SEM images of carbon coatings deposited a) in MS with Ne, b) in MS with Ar and c) by PECVD). All images are at the same magnification of 25000 and the scale-bar of 200nm is indicated.

A combination of NRA and SEM data was used to obtain the density of few carbon coatings produced in MS with Ne as discharge gas. The density of all the investigated coatings is lower than the nominal density of HOPG as shown in table 2. Four further coatings were investigated only by NRA/RBS (without ERDA) and for all of them the density was in the same range as presented here. Low values of density are not uncommon in carbon coatings prepared by MS as for instance in reference [23, 24].

Table 2: Data for the bulk composition and density from NRA measurements for 3 coatings deposited by MS and for HOPG. The value of the oxygen surface concentration has been added for comparison.

sample	**Density [g/cm^3]**	**δmax**	**O [at%]**	**H [at%]**	**Surface O[at%] by XPS**
CNe-a	1.5	0.97	11	19+/-2	8.9
CNe-b	1.4	0.97	11	13+/-2	11.8
CNe-c	1.4	Not measured	12	14+/-2	Not measured
HOPG (nominal)	2.3	1.23	0	0	0

In usual constant loss models for SEY curves the density influences the range of penetration of the primaries [25]. A lower density results in a larger range over which the energy of the primaries is dissipated. As a consequence only a small fraction of the generated secondary electrons reach the surface or are emitted. Thus in principle a lower density is expected to decrease the SEY. Such a model deals with a uniform solid. If the lower density of the carbon coating compared to HOPG is due to different length of bonds, missing bonds and internal stresses it can also be considered in average as a uniform solid. In this case the low density is consistent with the observed difference in SEY between HOPG and the carbon coatings deposited by MS. However, the low

density could also be due to porosity in a graphite-like matrix. In this case the lower value of the SEY compared to graphite could be explained by the scattering of secondary electrons to defects and pores, which would limit their mean free path and hence their capability to reach the surface and be emitted.

In addition the samples show a measurable content of oxygen and hydrogen in the bulk. For the analysis technique applied here the values are representative for a depth, which is larger than the escape depth of secondary electrons. Their possible influence is discussed in the next sections.

3.3 XPS and surface composition:

Many coatings were investigated with XPS just after the SEY measurement, by transfer through UHV. The main impurity detected on the surface is oxygen. Traces of N are occasionally found at a level below 1%. The presence of oxygen can be ascribed to the air exposure after deposition, but we cannot exclude that it is due to the level of oxygen present in the bulk, as detected by NRA. In particular for the two coatings where both techniques were applied the results are quite close (table 2). XPS measurements at grazing emission angle would possibly help to distinguish between surface and bulk contributions. Figure 4 shows the values of the oxygen concentration as measured by XPS and the resulting δmax values for various coatings. It is clear from the distribution that no correlation exists between the two quantities.

We conclude that the initial amount of oxygen does not influence δmax if its surface concentration is below 16%.

The line-shape of C1s of various types of coatings is presented in figure 5a and 5b. All the spectra are shown after subtracting the intensity at 281 eV and normalizing the curve with the maximum peak intensity. The spectrum of HOPG has a maximum at 284.4 eV,

with a very sharp and narrow line with a FWHM of 1.05 eV. A broader peak occurs around 291eV, which is typical of the $\pi \rightarrow \pi^*$ resonance in pure graphite.

***Table 3**: Summary of XPS data for all the coatings. The ratio in the last column is between the area of the two component s used for the fit (see text).*

sample	O concentration [at%]	FWHM [eV]	Ratio of Area(285.3 eV) over Area(284.4 eV)
CNe	2-16	1.5-1.7	0.18-0.26
CAr	3-12	1.7	0.24
PECVD	3-13	2	0.43
HOPG	0-0.8	1.1	1

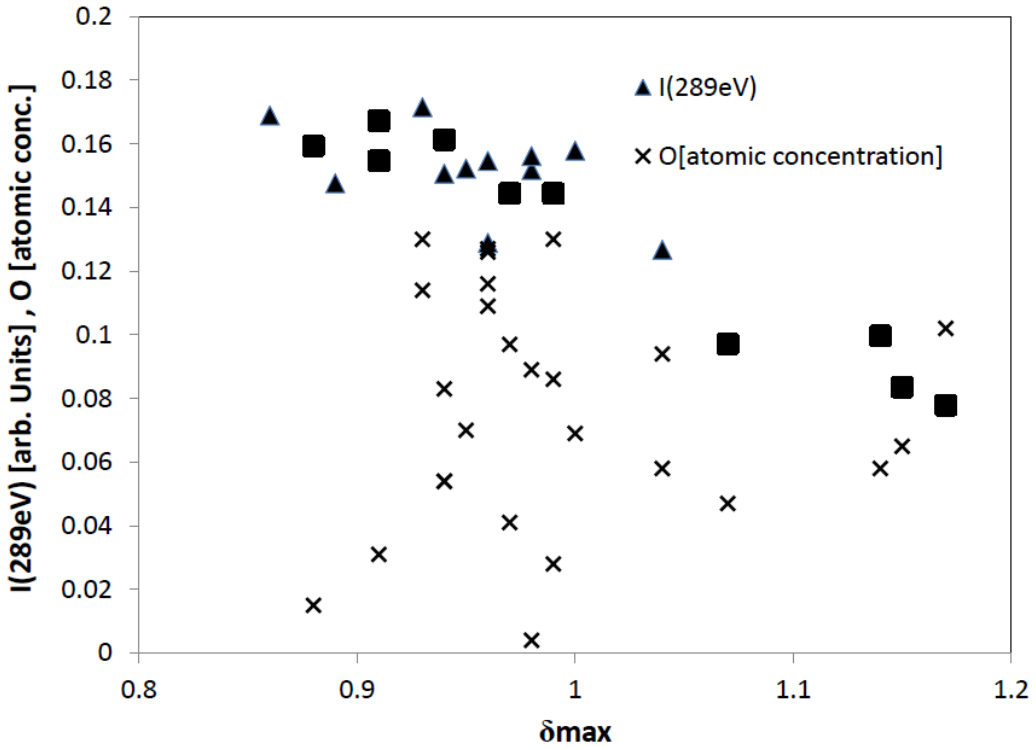

Figure 4: Surface concentration of oxygen (crosses) and intensity at 289eV (filled triangles and squares) measured for the various coatings as a function of the maximum SEY. Only MS coatings are included. The filled squares are from the same coating run as the data in figure 6.

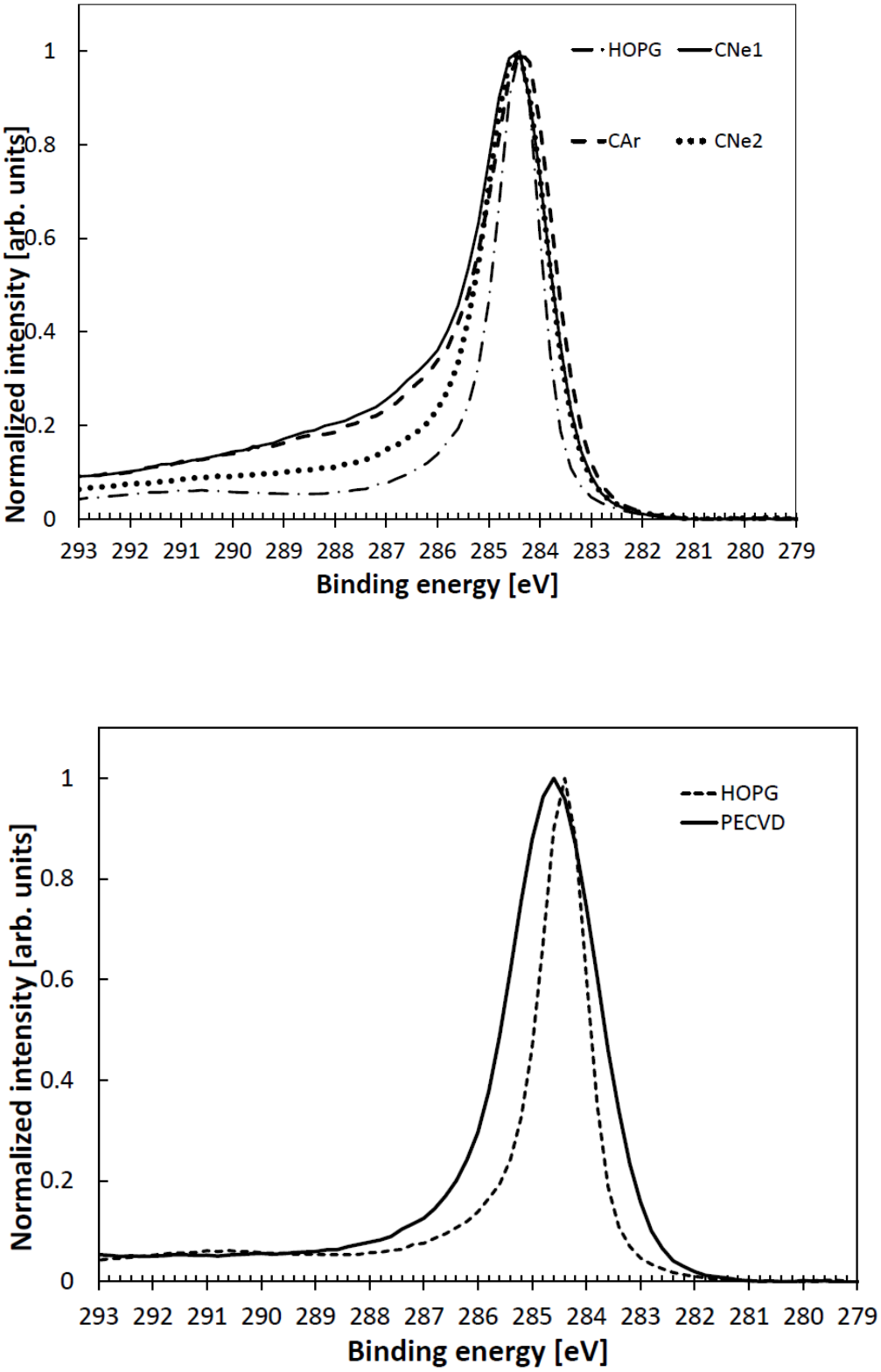

Figure 5 a) Example of two cases of C1s spectra of carbon coating deposited in MS with Ne (continuous line and dotted line) and Ar (dashed line) discharge gases, compared with HOPG (dashed dotted line). b) C1s line of PECVD (continuous line)

coating compared with HOPG (dotted line). The δmax for the MS coatings is 0.98 (dashed), 0.93 (continuous), 1.14 (dotted) and 1.5 for the PECVD coating.

The comparison between the C1s curves for HOPG and MS coatings immediately reveals a larger linewidth (table 3), whereas the energy shift is only about 0.1 eV, at the limit of the resolution of our spectrometer. Two quite different coatings were selected from the point of view of their δmax, without obvious relation to the coating parameters, which are within the range given in table I. The two cases shown in figure 5a for the Ne based coatings illustrate two extreme cases with a FWHM of 1.5 eV and 1.7eV. The C1s line for the PECVD coatings is shifted at 284.6 eV and is much wider (FWHM = 2eV).

The wider linewidth compared to HOPG is related to the presence of different species of bonds. These can be C-C bonds which have either another geometry or hybridization compared to the pure sp^2 of HOPG or belong to bonds of carbon to other chemical species. The latter can only be hydrogen, which is not detected directly by XPS, or oxygen.

In the case of PECVD one expects a larger amount of hydrogen in the coating than for MS due to the acetylene precursor, which has a 50% content of hydrogen. The binding energy for C-H bonds is shifted upwards by 0.65 eV [26] to 1.0eV [27] compared to a pure carbon sp^2 bond and the observed shift of 0.2 eV indicates an intensity increase of high binding energy components. Furthermore the presence of hydrogen is also known to favor the formation of sp^3 bonds [28], which have a 0.9eV shift toward higher binding energy compared to the sp^2 carbon [29]. The two effects, the presence of C-H bonds and sp^3 bonds cannot be distinguished through chemical shift. Adopting the analysis of reference 29 for the PECVD and MS samples we apply a fit from 281eV to

290 eV, including two components with 1.3eV FWHM at 284.4 eV, 285.3eV for sp^2 and sp^3, respectively. The residual intensity is compensated by three further components with 1.5eV FWHM at 286.5eV, 287.3eV and 288.3eV. Intensity in that region is generally justified with the presence of bonds of carbon with oxygen or by satellites deriving from the $\pi \rightarrow \pi^*$ transition [29]. We note that the intensity attributed to those components strongly depends on the width of the range which is selected for the fit procedure. The results of the ratio between the area of the component at 285.3eV and the one at 284.4 eV are presented in table 3. Following the interpretation of reference 29 it is clear that the PECVD coating has a larger amount of sp^3 bonds compared to the MS coatings. For the latter the coating is dominated by sp^2 bonds, with a fraction of about 30% of sp^3 bonds. However, the picture is very likely more complex, since the calculated ratio is influenced by the presence of hydrogen in different amounts in the various coatings and the effect of hydrogen and the abundance of sp^2/sp^3 cannot be disentangled just by XPS.

The only correlation between the XPS data of all the coatings and the resulting δmax or Emax involves the intensity on the high binding-energy side of the C1s line, as for instance at 289eV (the result is very similar by taking any point in the region 287-290 eV). In figure 4 the intensity at 289 eV is taken after subtracting the intensity at 281 eV – as for a constant background - in the same spectrum and normalizing the value by the C1s peak maximum to one. The result is shown in figure 4 as a function of the respective SEY of the coatings. The samples having a higher SEY exhibit a lower intensity in the 289 eV region. We do not have a definite explanation for this correlation and we considered the following arguments. The intensity on the high binding energy side of C1s can be given by i) bonds with other chemical species, ii) the $\pi \rightarrow \pi^*$ transition and more generally iii) electrons emitted at the energy of the main line which

undergo inelastic scattering before emission. Oxygen would be the best candidate to contribute to mechanism i), but the data in figure 4 show also that the oxygen concentration is correlated neither with the δmax nor with the intensity at 289eV. This discards the mechanism i). The presence of stronger intensity of the $\pi \rightarrow \pi^*$ transition - ii) – with a broad energy range of the transition due to the disordered structure of the material [29] would point toward a more pronounced sp^2 character fort the samples having a lower δmax and this is coherent with the lower δmax of the MS coatings compared to the PECVD and according to the ratio reported in table 3 if it is interpreted as the ratio of sp^3/sp^2. However, this situation is not consistent with the fact that HOPG has a low intensity in that region and, by definition, the highest possible sp^2 content.
The third proposed mechanism – iii) – encompasses a large amount of possible type of inelastic scattering mechanisms. The photoelectrons at a kinetic energy of about 970eV would suffer energy losses along the path to the surface and generate a high background as discussed in the model of Tougaard [30] for buried layer, impurities or surfaces covered by islands of different elements. However, in the present case the system is homogenous, constituted mostly of a single element, namely C. We did not find an application for instance to rough surfaces made of a single element. In addition higher losses imply that primary electrons release their energy in a shallower depth, exciting in that way secondary electrons close to the surface, which can in turn escape easily giving rise to a high SEY. This is at odds with the present experimental findings with a low δmax for the samples having high intensity at 289eV.
More experiments, for instance by varying the emission angle in XPS to verify the surface sensitivity of the high binding energy intensity, could possibly help to explain this effect.

3.4 Residual gas during coating

In figure 6 the δmax of a series of coatings produced in MS, all for the same chamber geometry, is shown as a function of the water and hydrogen content in the discharge gas, as determined from the RGA signal during coating. The presence of hydrogen and water is not due to impurities present in the original gas, as can easily be verified by injecting the gas without starting the discharge. It is due to degassing of the entire vacuum system including the chamber and the graphite cathode target. From the behaviour observed for hydrogen (figure 6a) it is easy to conclude that the SEY is influenced by the content of hydrogen during the discharge. The degassing pressure of water (figure 6b) remains about 10 times lower than for hydrogen, in a range where even hydrogen does not show a clear relation with the SEY. Thus if the water pressure during coating remains below the limits presented here it does not have an influence on the SEY. It is plausible that a higher amount of hydrogen in the plasma will result in a higher amount of hydrogen in the coating. The effect of increase of SEY due to the presence of hydrogen is consistent with previous studies. Indeed for hydrogen implanted in graphite, simulations [31] and experiments [32] conclude an increase of SEY. Preliminary tests of MS coatings produced by dosing hydrogen during the sputtering process are in progress and confirm this influence. The influence of hydrogen seems to be in contradiction with the single result in table 2, where two samples with different H content have the same δmax. On one hand we remark that the concentration measured by nuclear techniques is possibly not representative for the depth where the generation of secondary electrons occurs. This is particularly true for a gas like hydrogen, which is highly mobile. On the other hand the influence of hydrogen might start to be relevant for levels which are higher than those reported in table 2.

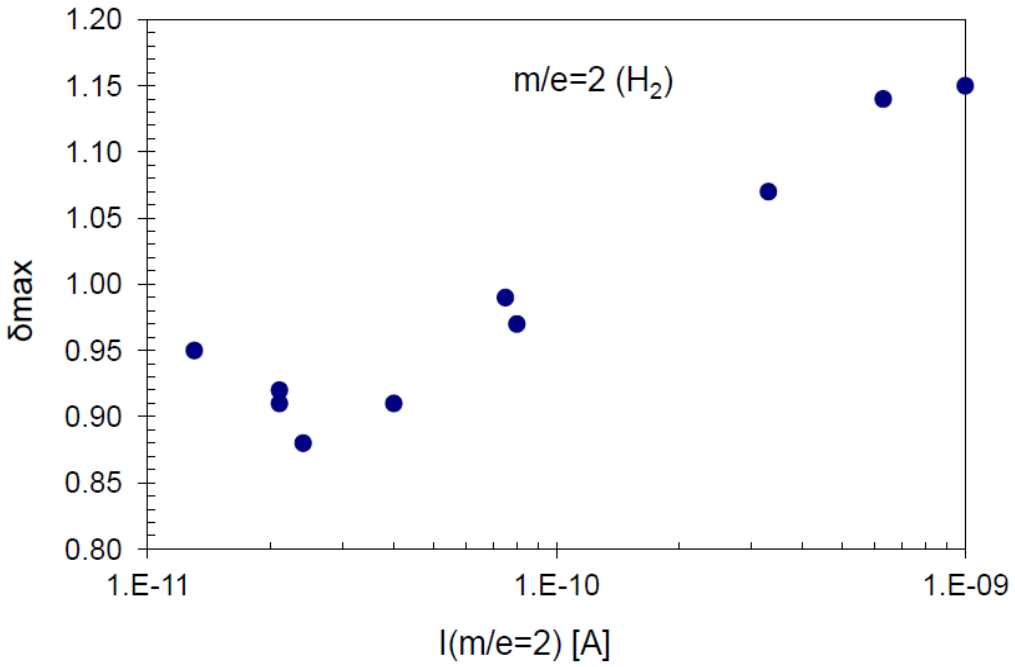

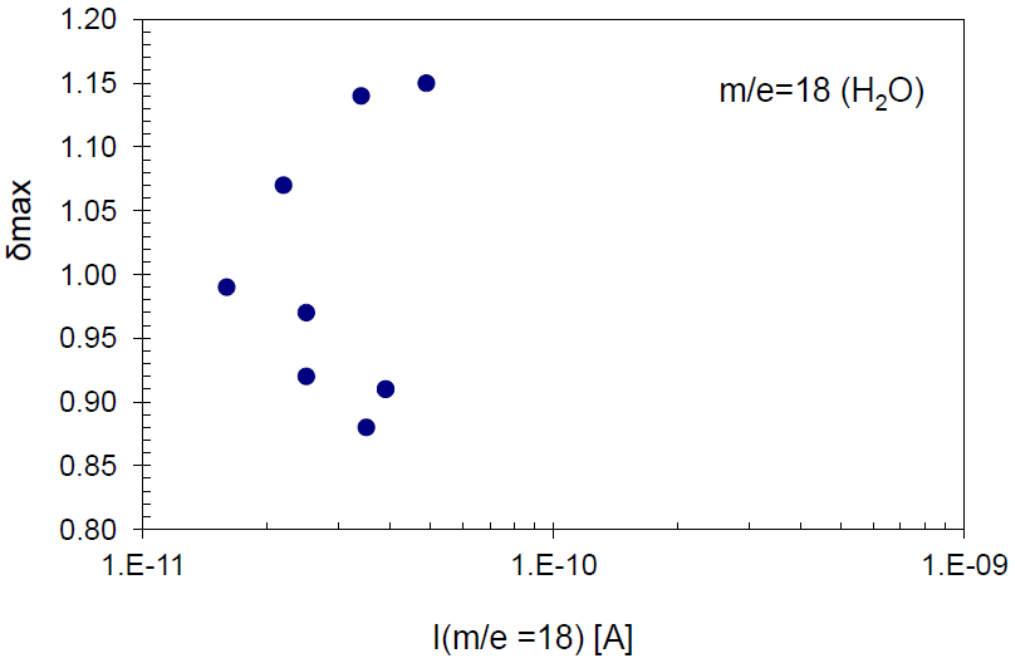

Figure 6 a) Resulting δmax for various coatings as a function of the RGA signal intensity for m/e=2 (H_2). b) The same as in part a, but as a function of the signal intensity at m/e=18 (H_2O)

4. Aging. Influence of the storage on SEY.

The motivation for the development of the carbon coatings was to produce a surface having a low SEY with a δmax around 1 and being sufficiently inert to preserve such a low value even after prolonged air exposure. This is of concern in the event of venting for maintenance, as it is the case for accelerators. The evolution of the δmax of identical coatings – from three coating runs in MS – stored in different environments is presented in figure 7.

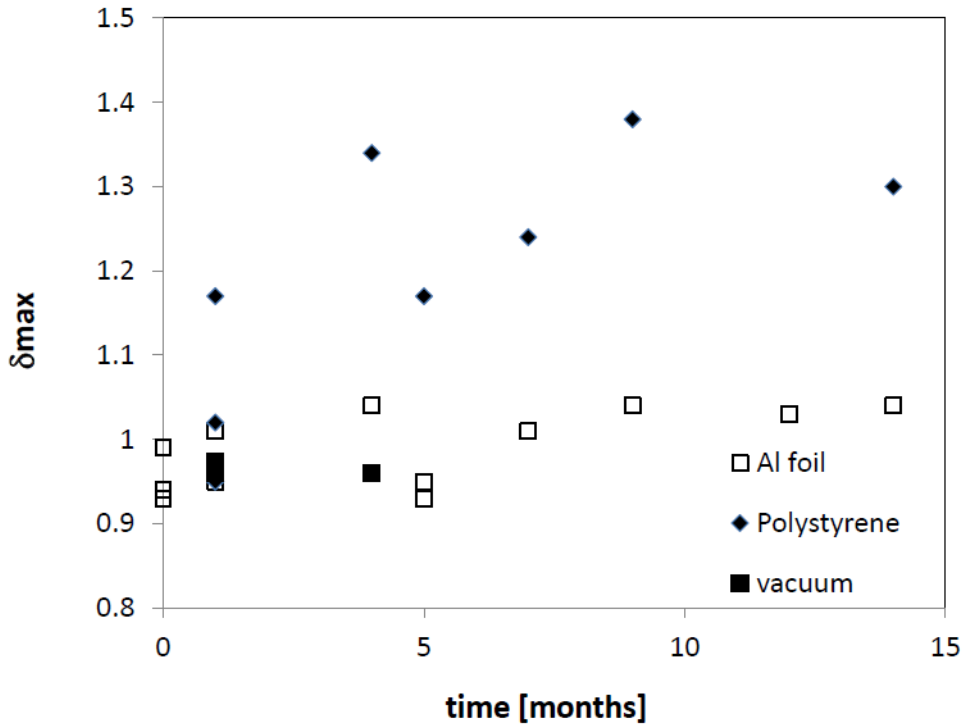

Figure 7: Evolution of δmax as a function of storage time in different conditions.

To prevent the macroscopic contamination with dust the coatings were stored either in a commercial polystyrene box in air, or wrapped in aluminium foil in air, or closed in a stainless steel chamber under static vacuum. The chamber was pumped down with a turbo-molecular pump and then separated by a closed valve. The increase of the δmax

for the samples stored in the polymer box is quite important after few months of storage. For the samples in vacuum and in aluminium foil the increase is at the limit of detection even after one year. Thus a very simple storage method is sufficient to protect the samples from deterioration even in air. It can easily be applied to vacuum chambers by closing their end flanges.

The next question concerns the reason for the deterioration observed for the storage in the polystyrene box. The XPS data reveal an increase of oxygen as main modification on the surface composition.

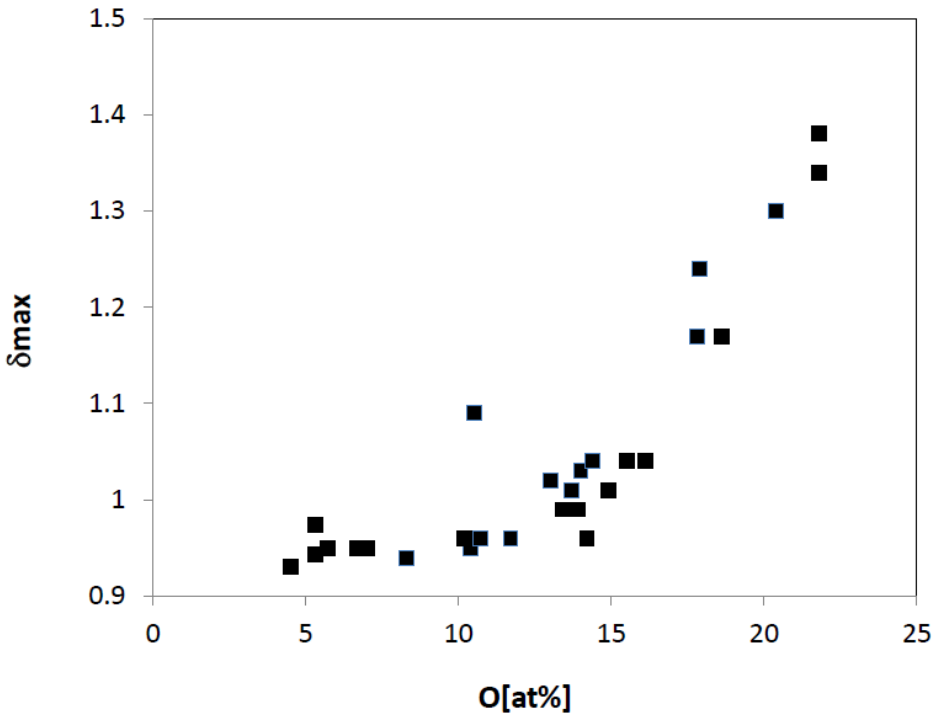

Fig. 8: Maximum SEY as a function of accumulated oxygen amount on the surface during storage

Figure 8 displays the resulting δmax as a function of the accumulated oxygen surface concentration, as measured by XPS. Data for all the storage times in all environments are included. The dependence observed in figure 8 indicates that the increase in oxygen

above about 15% atomic occurs simultaneously with the deterioration of the SEY. The oxygen O1s line has its maximum at 532.6eV before and after sample storage. This energy is compatible with the presence of airborne water and hydroxyls related species [33], but also -COO chemical species. The fact that no chemical shift or no marked change of the O1s lineshape is observed, leads to the conclusion that the chemical species of oxygen do not change during the storage time, but just increase in abundance. A careful analysis of the C1s line shows that no shift of the maximum does occur upon storage (figure 9), but for the samples stored in polystyrene the intensity increases weakly in the region of 288.5eV. In case of airborne contamination, this is generally identified as a contribution from -COO bonds [33]. In conclusion both, hydroxyls groups and hydrocarbons with -COO bonds adsorb on the surface during storage in polystyrene, whereas almost no change is observed for the sample stored wrapped in aluminum foil. Due to the strength of the main C1s line from the substrate it is not possible to ascertain whether any increase of CHx components occurs. In a previous study on copper surfaces [18] the stronger increase of the carbon signal upon storage in polyethylene compared to wrapping in aluminium foil was already demonstrated. This complex contamination layer formed by hydrocarbons and hydroxyls is the origin of the increase of the SEY as already observed on metallic surfaces [5].

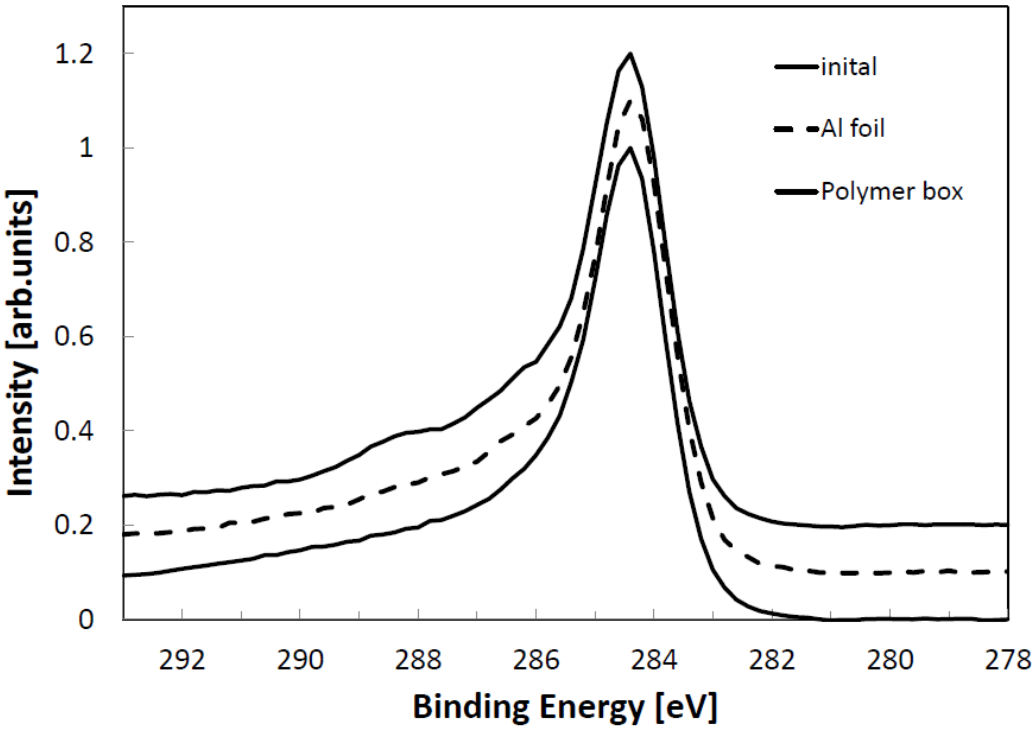

Figure 9: XPS spectra of the C1s line of a CNe coating just after production (continuous line), and after storage in aluminium foil (dashed line) and in a polystyrene box (thick continuous line)

5. Conclusions

The extended investigation of the SEY electron yield properties of carbon coatings demonstrates that the best method to achieve low δmax is deposition by MS compared to PECVD. More than 100 coatings prepared by MS exhibit a very narrow distribution of δmax around 1after few hours of air exposure and without annealing, cleaning or conditioning before measurement. This SEY is lower than for HOPG cleaved in air, probably because of the lower density and higher surface roughness of the coatings. The data demonstrate that the amount of H_2 in the discharge gas provoked by outgassing deteriorates the SEY of the resulting coating. The content of hydrogen is also very likely the reason of the worse results obtained by coating with PECVD in acetylene. In

contrast the surface concentration of oxygen in MS coatings does not influence the SEY result when below 16% atomic. The main correlation which has been found between the XPS data and the SEY data resides in the high intensity in the high binding-energy side of the C1s peak, which corresponds to a lower δmax of the surface.

The effect of storage on the value of δmax has been investigated for different conditions. Wrapping the samples in aluminium foil has been demonstrated to be sufficient to preserve the properties in air for more than one year. Instead storage in polystyrene boxes provokes a continuous increase of SEY with an increase of coverage by O and oxygen bearing hydrocarbons. This contamination layer deteriorates the properties of the coating. The storage in aluminium foil and static vacuum demonstrates that a simple method can be applied to store large vacuum chambers before installation in accelerator plants and short air exposure periods are not deleterious for the SEY properties. Such coatings have been successfully applied in small test chambers in proton accelerators [17] and in a radiofrequency multipacting test-bench [34] and in both cases they have demonstrated electron-cloud suppression. No major issues were encountered so far with the vacuum behaviour of those coatings, but a more precise quantitative evaluation of the outgassing will be carried out. The application of carbon coatings on a long test section of the SPS and later to a large part of the machine is foreseen.

Acknowledgments

We thank M.Scheubel and I. Aviles for SEM pictures, J.M.Jimenez and O.Teodoro for helpful discussions and the SPSU and LIU-SPS Project teams of CERN for continuous support.

References:

[1] A. N. Curren, NASA technical paper 2285 (1984) 13.

[2] J.M.Jimenez, G.Arduini, P.Collier, G.Ferioli, B.Henrist, N.Hilleret, L.Jensen, K.Weiss, F.Zimmermann, LHC Project report 632, 2003, CERN, Geneva;

[3] W. Fischer, M. Blaskiewicz, M. Brennan, H. Huang, H.-C. Hseu, V.Ptitsyn, T.Roser, P.Thieberger, D.Trbojevic, J.Wei and S.Y.Zhang, p.759, Proceedings PAC 2007, Albuquerque, USA

[4] C. Kunz, Synchrotron radiation overview, Photoemission in Solids II (1979) 322.

[5] N. Hilleret, C. Scheuerlein, M. Taborelli, Appl. Phys. A76 (2003) 1085–1091.

[6] M. Pivi, F. K. King, R. E. Kirby, T. O. Raubenheimer, G. Stupakov, and F. Le Pimpec, J. Appl. Phys. 104 (2008) 104904

[7] C. Scheuerlein, B.Henrist, N. Hilleret, M. Taborelli, Appl. Surf.Sci. 172 (2001) 95-102

[8] P.He, H.C.Hseuh, M.Mapes, R.Todd and D.Weiss, PAC2001 preoceedings, Chicago, (2001) 2159-2161

[9] P. Chiggiato, P. C. Pinto, Thin Solid Films 515 (2006) 382 – 388

[10] P.Prieto and R.E. Kirby, J.Vac.Sci.Technol. A13 (1995) 2819-2826

[11] I.Montero, S.H.Mohamed, M.Garcia, L.Galan and D.Raboso, J.Appl.Phys. 101 (2007) 113306

[12] E.G.Martsinoskaya, Soviet Physics Sol. Stat. 7 (1965) 661.

[13] N.R.Whetten, J.Appl. Phys. 34 (1963) 771 .

14] J. M. Ripalda, I. Montero, L. Vazquez, D. Raboso, L. Galan, J. Appl. Phys. 99 (4) (2006) 043513.

[15] M.Nishiwaki, S.Kato, Vacuum 84 (2010) 743-746

[16] C.Scheuerlein, M.Taborelli, N.Hilleret, A.Brown and M.A.Baker, Appl. Surf.Sci. 202 (2002) 57-67

[17] C. Yin Vallgren, G. Arduini, J. Bauche, S. Calatroni, P. Chiggiato, K. Cornelis, P. Costa Pinto, B. Henrist, E. Me´tral, H. Neupert, G. Rumolo, E. Shaposhnikova, and M. Taborelli, Phys. Rev. Special Topics, Acceleratorsand beams, 14 071001 (2011)

[18] C.Scheuerlein and M.Taborelli, Appl. Surf.Sci. 252 (2006) 4279.

[19] M. Mayer, Simra, a simulation program for the analysis of nra, rbs and erda,Vol. 475, AIP, (1999), 541–544.

[20] SIMTarget, http://www.fundp.ac.be/simtarget (2009).

[21] J. Moulder, W. Stickle, P. Sobol, K. Bomber, Handbook of X-ray spectroscopy, Perkin-elmer, Eden Prarie, Minnesota, USA, 1992.

[22] I. Bojko, N.Hilleret, C.Scheuerlein, JVST A18 (2000) 972-979

[23] L.G. Jacobsohn, F.L. Freire, J.Vac.Sci.Technol A17 (1999) 2841.

[24] E.Mounier, F.Bertin, M.Adamik, Y.Pauleau, P.B.Barna Diamond an Related Materials 5 (1996) 1509.

[25] A.J. Dekker, Solid State Physics, ed. F. Seitz, D. Turnbull, H. Ehrenreich, Academic Press, NY, Vol VI, 251 (1958)

[26] A.Nikitin, L.A. Naslund, Z.Zhang and A.Nilsson, Surf.Sci. 602 (2008) 2575.

[27] P.Ruffieux, O.Groening, P.Schwaller, L.Schlapbach and P.Groening, Phys.Rev.Lett. 84, (2000) 4910.

[28] J. Robertson, Material Science and Engineering R37 (2002) 129-281.

[29] S.T.Jackson and R.Nuzzo, Appl. Surf.Sci. 90 (1995) 195.

[30] S.Tougaard, Surf.Sci. 216 (1989) 343-360

[31] K.Nishimura and K.Ohya, Jpn. J.Appl. Phys. 32 (1993) 2856.

[32] M.E.Woods, B.Hopkins, G.F.Matthews, G.M. McCracken, P.M.Sewell and H.Fahrang, J.Phys. D: Appl. Phys. 20 (1987) 1136.

[33] M.Mantel and J.P.Wightman Surf. Interf. Anal. 21 595-605 (1997)

[34] P. Costa Pinto, F. Caspers, P. Edwards, M. Holz, M. Taborelli, Proceeding of IPAC12, New Orleans, accepted for publication